Tectonostratigraphy of the Khoy Complex, northwestern Iran

Emile A. Pessagno, Jr.[1], A. Mohamad Ghazi[2], Mohsen Kariminia[1], R. A. Duncan[3], and A. A. Hassanipak[4]

[1]*Department of Geological Sciences, The University of Texas at Dallas, PO Box 830688, Richardson, TX 75083-0688*
[2]*Department of Geology, Georgia State University, Atlanta, GA 30303*
[3]*COAS, Oregon State University, Corvallis, OR 97331-5503*
[4]*Department of Mining Engineering, University of Tehran, Iran*
email:pessagno@utdallas.edu

ABSTRACT: Previous studies suggested that only one ophiolite, the "Khoy ophiolite", existed near Khoy, northwestern Iran. This thesis is no longer tenable.

Combined investigations (biostratigraphic, chronostratigraphic, geochonometric, geochronologic, and geochemical) demonstrate that there are at least two and perhaps three ophiolite remnants in the Khoy area:

(1) A Late Jurassic (early to middle Oxfordian: 156 Ma to 159 Ma ^{40}Ar-^{39}Ar on gabbro) remnant;

(2) A Late Cretaceous (early Coniacian: Radiolaria) remnant (~N-MORB geochemistry); and, possibly,

(3) A Late Cretaceous (latest Campanian) remnant (E-MORB geochemistry).

Because it is impossible to use the term "Khoy ophiolite" in this report, we refer the ophiolitic rocks in the Khoy area to the "Khoy Complex" (sensu International Stratigraphic Guide).

The sedimentary contact between Late Cretaceous (early Coniacian) red manganiferous ribbon chert lacking calc-alkaline volcanic contributions and overlying pyroclastics (tuff and tuff breccia) in the far northwestern part of the Khoy complex is of great tectonostratigraphic significance. This interface represents a sudden change from pelagic to pyroclastic sedimentation. Field evidence indicates that the contact is disconformable and is associated with a hiatus of unknown magnitude. Red ribbon chert (lacking calcalkaline contributions) in the same area overlies and is interbedded with N-MORB pillow basalt; early Coniacian Radiolaria were recovered from interpillow siliceous mudstone. We postulate that by the early Coniacian oceanic crust (covered with a veneer of Radiolarian ooze) had moved close enough to an island arc system to receive calc-alkaline pyroclastics.

Tectonic mélange in the Khoy Complex represents a subduction complex probably associated with the island arc noted above. Micrite (pelagic limestone) knockers in the tectonic mélange belt contain Early Cretaceous (late Albian: Vraconian) planktonic foraminifera; Late Cretaceous (early Cenomanian) Radiolaria; Late Cretaceous (early Campanian to early Maastrichtian) planktonic foraminifera; Late Cretaceous (late Maastrichtian) planktonic foraminifera; and early Middle Eocene planktonic foraminifera. The age of the micrite knockers in the tectonic mélange, suggests that subduction associated with island arc volcanism continued from the Early Cretaceous (latest Albian) to the Early Tertiary (early middle Eocene).

INTRODUCTION

The geological evolution of southern and western Iran can, in part, be characterized by accretionary tectonics where tectonostratigraphic terranes of different origins are now juxtaposed. Although the origin of most of these terranes can be traced back to continental margins of Eurasia or the Afro-Arabian plate, other terranes contain numerous ophiolites (text-figures 1-2) of oceanic affinity and represent fragments of accreted Tethyan ocean crust on continental margins (e.g., Dewey and Bird 1970; Moores and Vine 1971; Coleman 1981; Nicolas and Boudier 1991).

Iranian ophiolites have been divided into four groups (Takin 1972; Stocklin 1974; see text-figure 2):

1) Ophiolites of northern Iran along the Alborz range;

2) Ophiolites of Bitlis-Zagros Suture Zone including the Neyriz and the Kermanshah ophiolites which appear to be an extension of the Oman ophiolite abducted onto the Arabian continental mass;

3) Ophiolites and colored tectonic mélanges of Makran which are located to the south of the Sanadaj-Sirjan microcontinent including unfragmented complexes such as Sorkhband and Rudan; and

4) Ophiolites and colored mélanges that mark the boundaries of the internal Iranian microcontinental block including some of those in the Makran region (e.g., Band-e-Zyarat, Dar Anar, Ganj) and those inside of the Sanadaj-Sirjan microcontinental block (Baft, Nain, Shar-Babak, Sabsevar and Tchehel Kureh).

The Khoy area is situated near an important junction where the Iranian ophiolites connect with the Turkish and Mediterranean ophiolites (text-figs. 1-3). Curiously, the ophiolites of the Khoy area have been entirely overlooked in the widely accepted tectonic model for the origin of Middle Eastern ophiolites and the closure of the Tethyan Ocean (Moores et al. 1984; Dilek and Delaloye 1992; Dilek and Moores 1990; Sarkarinejad 1994).

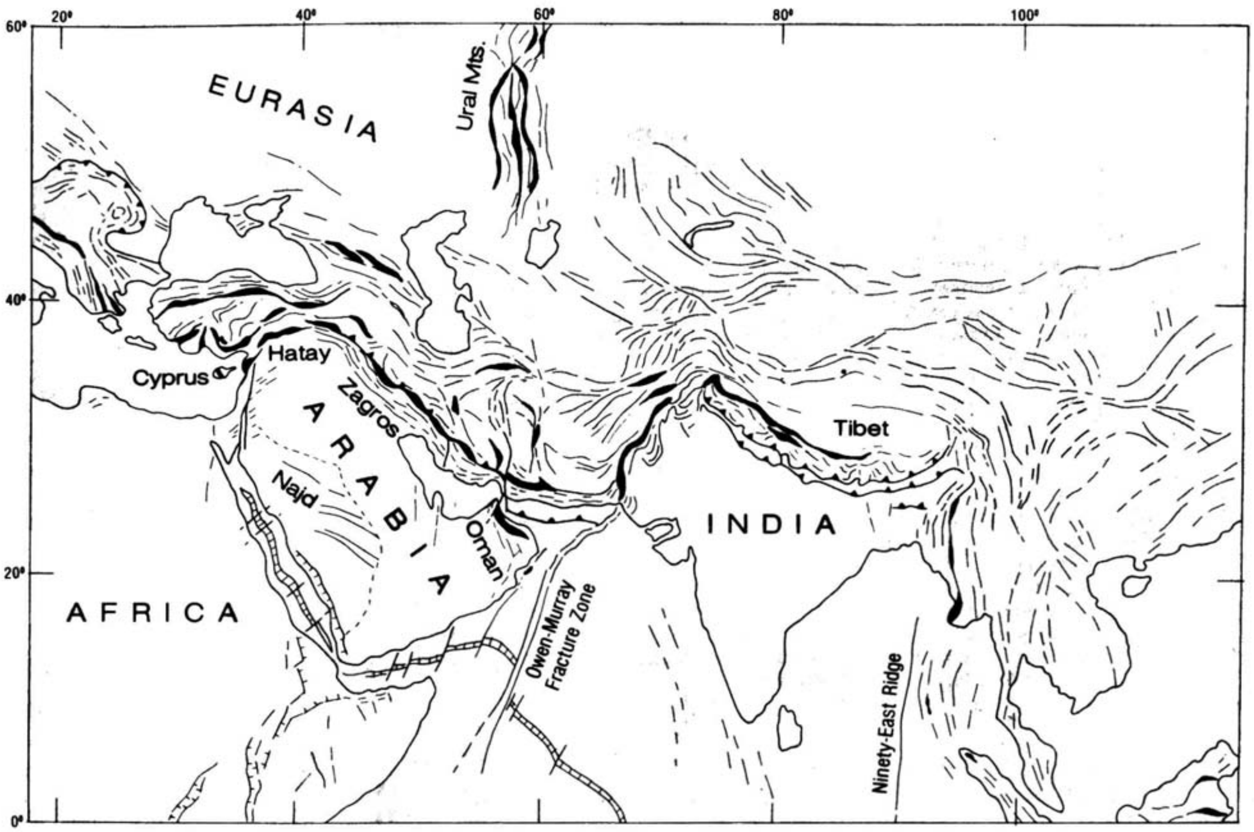

TEXT-FIGURE 1
Generalized tectonic map showing distribution of ophiolites along Tethys suture. Black areas include ophiolites and colored mélange zones. From Coleman (1981).

According to this model the ophiolites of the Bitlis-Zagros Suture Zone [Troodos (Cyprus), Baer-Bassit (Syria), Hatay, Kizildag and Cilo (Turkey), Kermanshah, Neyriz and Esphandagheh (Iran) and Samail (Oman)] may represent ridge segments of an ancient "ridge-transform fault" oceanic spreading axis that was located in the southern Tethys and was connected to what are now the Troodos and Samail ophiolites. Previous analysis of radiolarian chert samples by the senior author of samples (Paragon Oil Company) from the Kermanshah Ophiolite yielded the same Upper Cretaceous (lower Coniacian) radiolarian assemblage as that which occurs in the northwest part of the Khoy area associated with N-MORB pillow basalt (Localities Kh-01-D3-S22 and Kh-01-D3-S24, Table 1; Figure 3, "E"). It is tempting to suggest that this ophiolitic remnant within the Khoy is closely related to the Kermanshah Ophiolite. Geochemical studies by Ghazi (in progress) may be useful in confirming this relationship.

Earlier reports (e.g., Ghorashi and Arshadi 1978) suggested that only one ophiolite, the "Khoy ophiolite", occurred in the area near Khoy, northwestern Iran. This thesis is no longer tenable. Our preliminary studies of the Khoy region indicate that this area is complicated structurally and contains remnants of ophiolitic and island arc rocks of different ages and different origins. Hence, the term "Khoy ophiolite" can not be accurately applied in the Khoy area. In this report the term "Khoy Complex" (sensu International Stratigraphic Guide) is applied to the rocks in the area of study.

Previous investigations dealing with the "Khoy complex" (e.g., Ghorashi and Arshadi 1978) contained sparse biostratigraphic and chronostratigraphic data. An initial objective of the present investigation was to obtain radiolarian and planktonic foraminiferal biostratigraphic and chronostratigraphic data from volcanic rocks that have been mapped as ophiolite within the "Khoy complex" as well as from strata that occur in contact (sedimentary or fault) with ophiolitic rocks within the "Khoy complex". Where possible, we have integrated the new biostratigraphic and chronostratigraphic data with both new and existing geochronometic and geochemical data. Samples for geochemical analysis were collected in conjunction with micropaleontological sampling. All new samples were located using a handheld global positioning unit (GPS).

REGIONAL GEOLOGY

The "Khoy complex" is bounded to the west and north by the Iran-Turkey border and to the east by a northwest-southeast trending fault (text-figure 2). To the south the "Khoy complex" is in contact with the northern edge of the Sirjan-Sanandaj Zone. The Cretaceous rocks, which include the "Khoy complex", constitute two-thirds of all the outcrops in the area. Our investigations, thus far, have produced biostratigraphic, chronostratigraphic, geochronometric, geochronologic, and geochemical data from four areas within the "Khoy complex" (text-figs. 3-4):

Area 1: A Lower Cretaceous (early Albian) amphibolite closely associated with an Upper Jurassic (lower Oxfordian

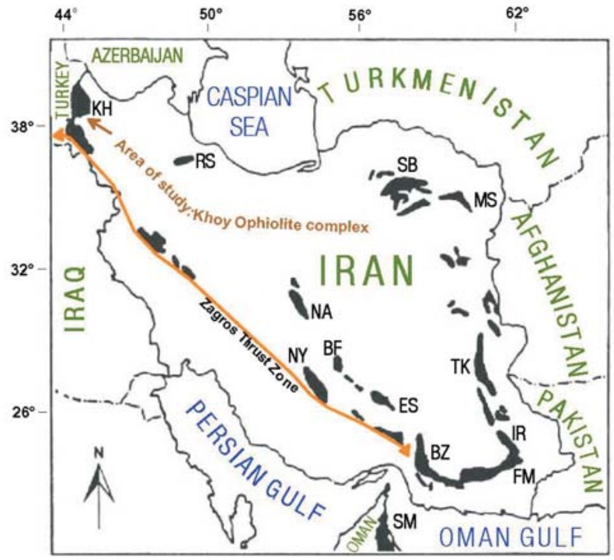

TEXT-FIGURE 2
Sketch map of Iran showing locations of most important ophiolites. KH = Khoy; KR = Kermanshah; NY = Neyiz; BZ = Band Ziarat; NA = Nain; BF = Baft; ES = Esphandagheh; FM = Fanuj-Maskutan; IR = Iranshahr; TK = Tchehel Kureh; MS = Mashhad; SB = Sabzevar; RS = Rasht; SM = Samail.

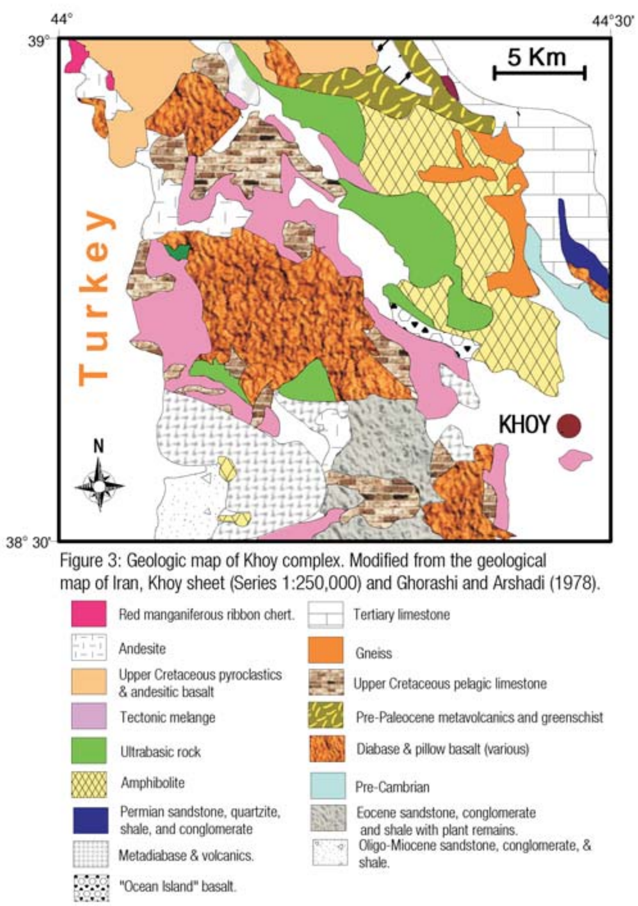

TEXT-FIGURE 3
Geologic map of Khoy complex. Modified from the geological map of Iran, Khoy Sheet (Series 1: 250,000) and Ghorashi and Arshadi (1978).

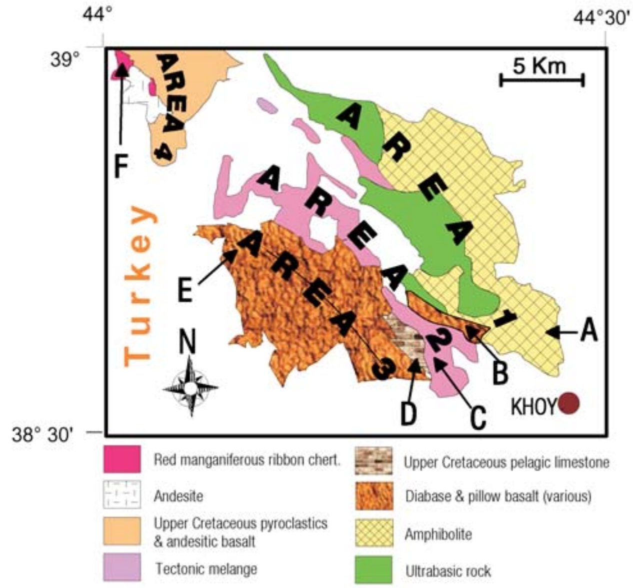

TEXT-FIGURE 4
Biostratigraphic, chronostratigraphic, geochronologic, and geochemical data from Areas 1-4.
Area 1: Early Cretaceous (earlier Albian) amphibolite + Late Jurassic (early to middle Oxfordian) remnant with ultramafics, gabbro. Amphibolite mass too large to represent metamorphose sole of Jurassic remnant. May represent another ophiolite remnant. No sedimentary rocks known.
Area 2: Tectonic melange containing knockers of pelagic limestone (micrite with Radiolaria and planktonic foraminifera), serpentenite, and basalt. Pelagic limestone knockers in melange ranging in age from Early Cretaceous (late Albian) to Early Tertiary (Early Middle Eocene). **"B" (below)** denotes the approximate position of samples displaying OIB (ocean island basalt geochemistry. These extrusive rocks may also represent a large knocker in the tectonic melange. This hypothesis is supported by the fact that the OIB is adjacent to the tectonic melange in Area 2.
Area 3: E-MORB basalt with interbedded pelagic limestone (micrite) containing Late Cretaceous (latest Campanian) planktonic foraminifera Basaltic andesite-subalkaline basalt pillow lava (N-MORB affinity) with interpillow siliceous mudstone containing Late Cretaceous (early Coniacian) radiolaria.
Area 4: Late Cretaceous (early Coniacian) red, manganiferous ribbon chert overlain disconformably by medium to thick bedded pyroclastics. Basal partof pyroclastic unit consists of conglomerate with red chert clasts which rests disconformably on underlying red ribbon chert unit. A = Samples yielding 40AR39AR data from this general area. B = Samples with ocean island basalt geochemistry. C = Micrite samples with late Albian (Vraconian), early Cenomanian, early Campanian, early Maastrichtian, late Maastrichtian, early Middle Eocene planktonic foraminifera and radiolaria D = Micrite samples with early Campanian to early Maastrichtian planktonic foraminifera directly associated with E-MORB basalt. E = Basaltic andesite- subalkaline basalt with signature similar to N-MORB. Interpillow siliceous mudstone yielding early Coniacian radiolaria. F = Red ribbon chert yielding early Coniacian radiolaria.

---

to middle Oxfordian) ophiolite remnant with gabbro, diabase, and ultramafics (Figure 4, "A"). No sedimentary rocks known.

a. Lower Cretaceous (Albian) amphibolite (Figure 4, Area 1,"A".):

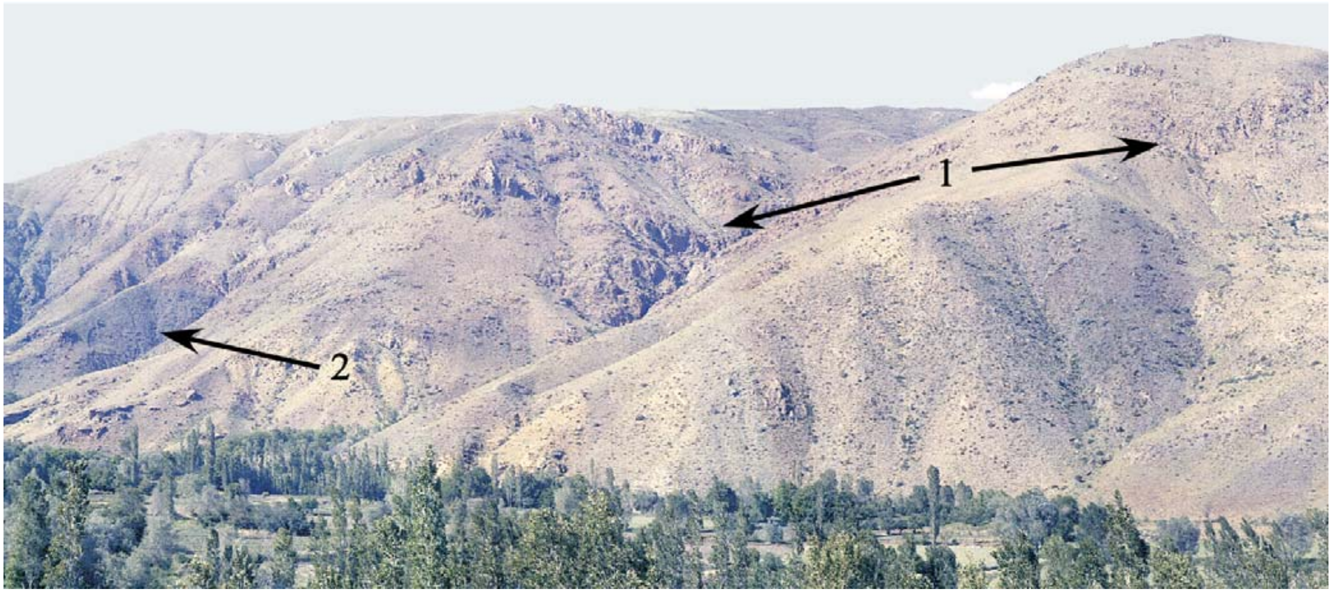

TEXT-FIGURE 5
View of tectonic mélange on west side of Area 2 (text-fig. 4). Arrows point to knockers of pink pelagic limestone (1) and basalt (2).

A large mass of amphibolite occurs in the eastern part of the Khoy Complex (text-fig. 4, Area 1 "A"). The western portion of the amphibolite is in tectonic contact with the ultramafic rocks and some of the lower gabbros units of the Upper Jurassic ophiolite whereas the eastern portion of the amphibolite unit is in contact with the Pre-Cambrian rocks (Kahar Formation). The rocks of the metamorphic zone show the effect of an inverse thermal gradient from amphibolite facies (e.g., hornblendite, gneiss and calc-silicate marble) immediately adjacent to the basal tectonized ultramafic rocks, to green schist facies (e.g., quartzite, phyllites, mica and chlorite-epidote schist) in contact with the Precambrian rocks.

The amphibolite is generally laminated, some having schistose and gneissic texture that show compositional layering consisting largely of brown-green hornblende and lesser amounts of plagioclase and quartz. Grain size ranges from less than 1mm to 10-15mm in finer-grained rocks to 1cm to 2-5cm in coarser-grained rocks. The highest grade amphibolites have gneissic texture and contain deformed layers, augen, and pods of coarse-grained plagioclase.

The Early Cretaceous (early Albian) amphibolite unit needs further investigation. It may represent an exotic slab that is unrelated to the adjacent Upper Jurassic ophiolite. It is probably too extensive to represent the metamorphose sole of the Upper Jurassic ophiolite.

b. Upper Jurassic (lower Oxfordian to middle Oxfordian) ophiolite remnant with gabbro, diabase, and ultramafics:

The Upper Jurassic gabbro is interpreted as cumulate gabbro and occurs as a small mapable unit adjacent to the basal amphibolite-gneiss. In general, the cumulate gabbro is massive, fine- to coarse-grained, and consists of clinopyroxene, plagioclase and olivine. Coarse-grained gabbros commonly contain large pegmatoid segregations and veins, up to 3-5cm grain size, which have contacts with the finer-grained host rocks that range from diffused and gradational to sharp and cross-cutting. The mineralogy of the pegmatoid gabbro consists of hornblende and plagioclase. In some areas, the gabbro contains patches of finer grained leucogabbro and diorite which have been mostly altered to greenschist facies assemblages of uralite; saussuritized plagioclase, epidote, and chlorite.

A diabase dike complex occurs within the Upper Jurassic remnant (text-figure 4, Area 1). The diabase dike complex within the Jurassic remnant is not as extensive as dike complexes in Semail or Troodos ophiolites, and because of extensive weathering it is difficult to identify any geometric relationships among individual dikes. The primary minerals of the dikes are of calcic plagioclase, clinopyroxene and Fe-Ti oxide. However, in most areas, the primary minerals have been completely replaced by alteration minerals that include actinolite, chlorite, epidote, prehnite, pumpellyite, quartz, and calcite.

The ultramafic sequence consists of two main rock types, harzburgite (70-80%) and dunite (20-30%,), which have been variably serpentinized and tectonized. Harzburgite consists of olivine (70-80%); orthopyroxene (20-30%); and Cr-spinel (1-2%).

Area 2: Tectonic mélange containing knockers of pelagic limestone (micrite with Radiolaria and planktonic foraminifera), serpentinite, and basalt.

Lower Cretaceous (upper Albian) to Lower Tertiary (lower middle Eocene) micritic limestone knockers occur in the tectonic mélange.

It should be noted that this area was mapped as a fault bounded block comprised mostly of pink pelagic limestone, basaltic lava flows, and colored shales by Radfar and Amini (Khoy Sheet, Geologic Map of Iran 1:100,000 Sheet 4967).

Text-figure 5 shows a panoramic view of hills along the western margin of Area 2 with knockers of pink pelagic limestone (micrite) and basalt in the mélange.

TEXT-FIGURE 6
N-MORB pillow basalt and red chert. See text-figure 4, "E". Arrow points to chert.

Area 3: Basalts with E-MORB AND N-MORB affinities.

E-MORB basalt with interbedded pelagic limestone (micrite) containing Upper Cretaceous (latest Campanian) planktonic foraminifera occurs at "D" in Area 3. (See Figure 4 and Geochemistry herein). Basaltic andesite-subalkaline basalt pillow lava (N-MORB affinity) with interpillow siliceous mudstone and red chert containing Upper Cretaceous (lower Coniacian) Radiolaria at "E" in Area 3 (See text-figure 4 and Geochemistry herein). Text-figure 6 shows spectacular pillow basalt near "E". Note the red chert overlying the basalt.

Area 4: Upper Cretaceous red, manganiferous ribbon chert overlain disconformably by conglomerate with well rounded chert clasts followed by medium to thick bedded pyroclastics (tuff).

To date, only lower Coniacian Radiolaria have been recovered from chert exposures adjacent to and below the pyroclastics. Text-figure 7 shows the disconformable contact between the red ribbon chert unit and the overlying pyroclastic unit.

These four areas form a framework for the discussion of and the interpretation of all data presented below.

BIOSTRATIGRAPHIC AND CHRONOSTRATIGRAPHIC DATA

New biostratigraphic and chronostratigraphic data resulting from our studies of Radiolaria and planktonic Foraminifera comes from Areas 2-4 above (see text-figure 4).

Area 2 (text-fig. 4): Tectonic mélange belt.

To date, we have recovered uppermost Albian (Vraconian); lowermost Cenomanian; lower Campanian to lower Maastrichtian; upper Maastrichtian; and lower Middle Eocene microfossil assemblages from micritic limestone knockers in the unnamed tectonic mélange belt. The results from our investigations are as follows:

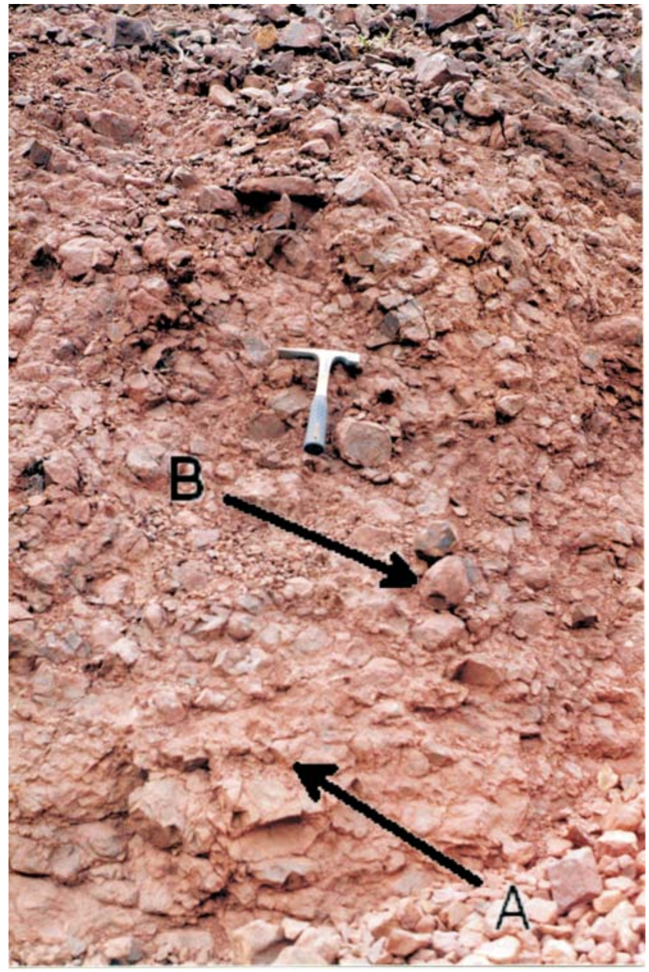

TEXT-FIGURE 7
Disconformable contact between red ribbon chert unit and pyroclastic unit Area 4, "F". See text-figure 4. "A" points to disconformable contact between red ribbon chert unit and overlying pyroclastic unit. A conglomerate with clasts of underlying chert unit occurs at the base of the pyroclastic unit. "B" points to clast in basal conglomerrate.

(1) A Lower Cretaceous (uppermost Albian) to Upper Cretaceous (lower Cenomanian) planktonic foraminiferal assemblage with *Thalmanninella evoluta, Hedbergella planispira,* and *Hedbergella delrioensis* occurs in micrite samples from Locality KH 99-46.3 (*See* Table 1; Area 2, "C" in text-fig. 4). This assemblage is assigned to Superzone 7 to Superzone 6, Zone 6D of Pessagno (text-figure 9).

(2) An Upper Cretaceous (lower Cenomanian) radiolarian assemblage with *Pseudodictyomitra pseudomacrocephala, Archaeodictyomitra sliteri, Holocryptocanium astiensis, Thanarla praeveneta, Patelula* spp., and *Alievium* spp. also occurs in micrite samples from Locality KH 99-46.3 (*See* Table 1; Area 2, "C" in Figure 4). The radiolarian assemblage is assignable to Zone 10, Subzone 10A (base) of Pessagno (1976, 1977; *see* Table 1 and text-figure 11 herein). The combined radiolarian and planktonic foraminiferal biostratigraphic data from Locality KH 99-46.3 indicate that micrites are assignable to the Upper Cretaceous (lower Cenomanian) and possibly the Lower Cretaceous (uppermost Albian).

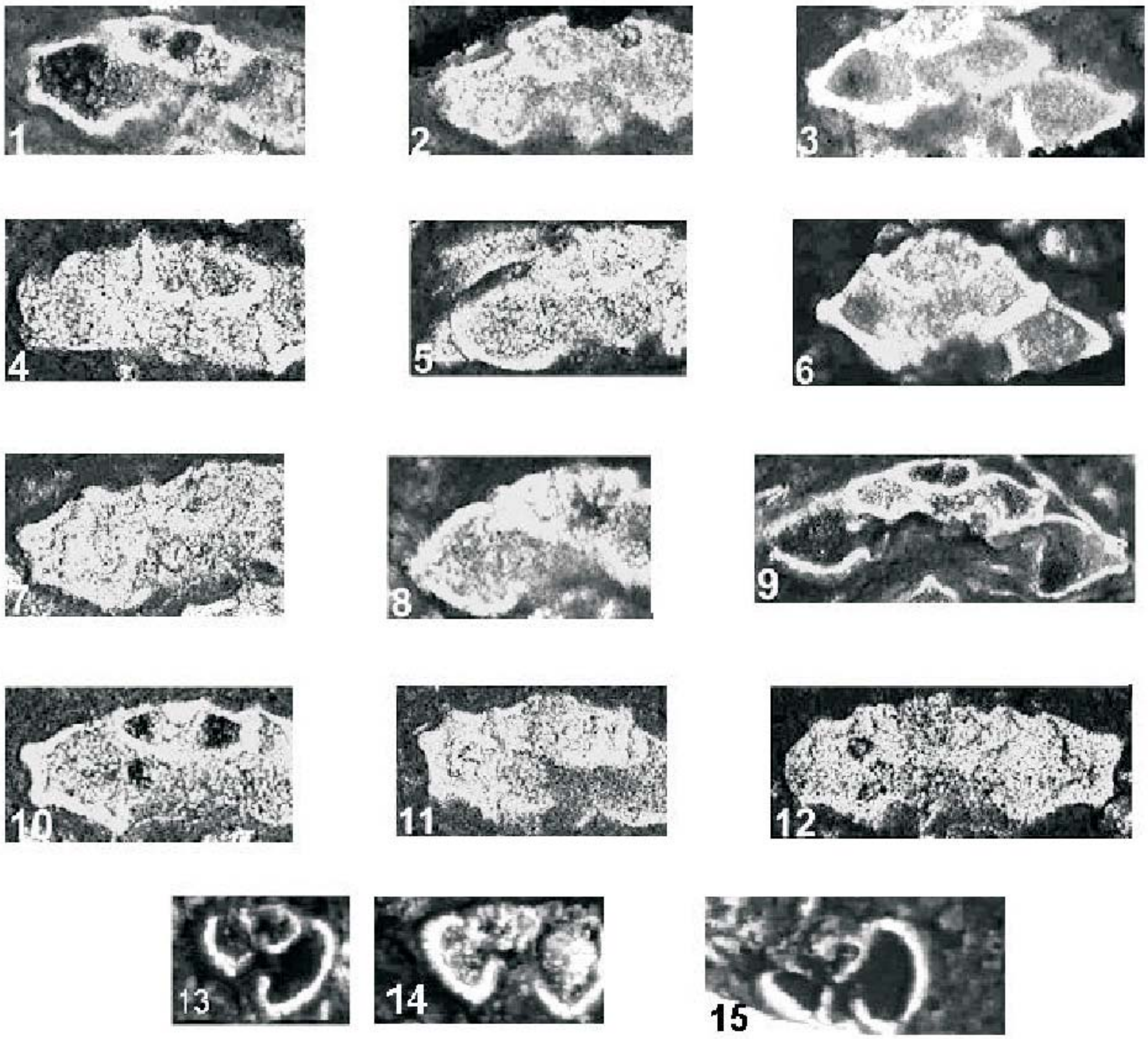

TEXT-FIGURE 8
Upper Cretaceous and Middle Eocene planktonic foraminifera from pelagic limestone (micrite) knockers in tectonic mélange. *See* Area 2, text-figure 4

Radiolaria were originally extracted from a micrite sample using concentrated HF (*See* Pessagno 1977, p. 7). One year after this sample was processed in concentrated HF co-author S. M. Kariminia developed his new acetic acid technique for extracting calcified radiolaria and other calcareous microfossils from micrites (Kariminia et al., 2003; Kariminia in press).

(3) Upper Cretaceous (lower Campanian to lower Maastrichtian) planktonic foraminifera including *Globotruncana linneiana, Globotruncana bulloides,* and *Globotruncana* spp. were identified from thin-sections of micrite from Locality Kh-01-D3-S19-b (Area 2. "C" in text-figure 4; Table 1). GPS coordinates are given for this locality in Table 1. This assemblage is broadly assigned to Zone 2 F (lower Campanian) to Zone 2A, Subzone $2A_1$ (lower Maastrichtian) of Pessagno (text-figure 10A). Planktonic foraminifera were identified from thin-section analysis of a micrite sample.

(4) Upper Cretaceous (upper Maastrichtian) planktonic foraminifera occurring in micrite from Locality Kh-01-D4-S29 were identified both from thin-section analysis and from matrix free specimens extracted from the rock using the acetic acid method (Kariminia et al. 2003; Kariminia in press). Taxa include *Globotruncanita conica, Globotruncanita elevata, Globotruncana navarroensis, Globotruncanella havanaensis,* and *Racemiguembelina fructicosa* (Area 2. "C" in Figure 4; Table 1). GPS coordinates are given for this locality in Table 1. This assemblage can be precisely assigned to Superzone K1, Zone 1B, base of Subzone $1B_1$ to Zone 1A. Both *Globotruncanita conica* and *Racemiguembelina fructicosa* (sensu

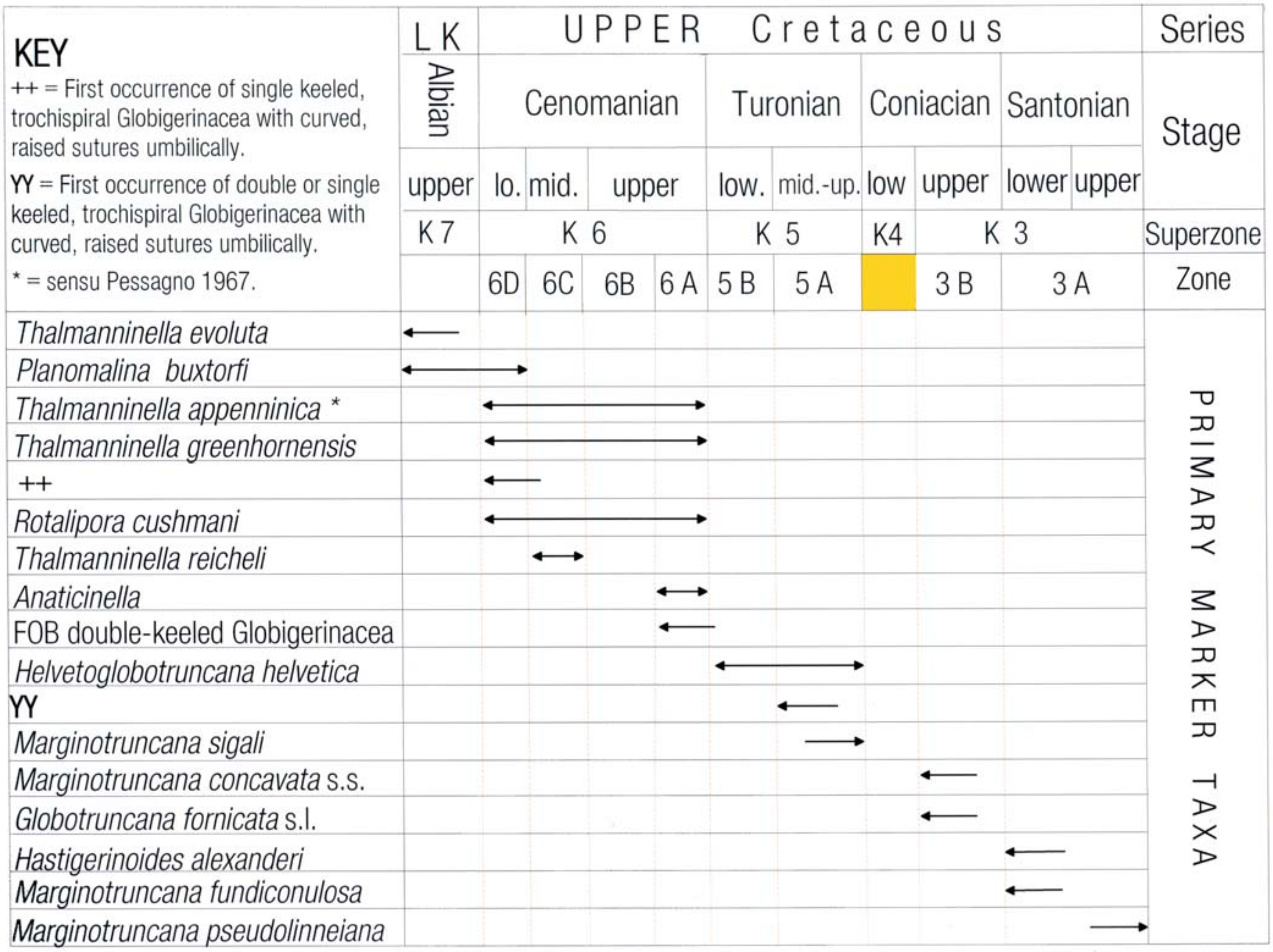

TEXT-FIGURE 9
Planktonic foraminiferal zonation for Cretaceous (part). Pessagno in prep. Note that K7 includes the Vraconian of older literature.

Smith and Pessagno 1972) make their first appearance at the base of part Subzone $1B_1$ in North America (e.g., Corsicana Formation, Texas: Pessagno 1967, 1969; Smith and Pessagno 1972. Text-figures 10A and 10B herein). It should be noted that Subzone $1B_1$ is equivalent to the *Racemiguembelina fructicosa* Zonule of Smith and Pessagno (1972, Figure 3).

(5) Lower Tertiary (Lower Middle Eocene) planktonic foraminifera were identified in thin-section analysis of micrite samples from Locality KH-99-21-1-2 (Area 2. "C" in text-figure 4; Table 1). Taxa from Locality KH-99-21-1-2 include *Acarinina densa* and *Acarinina* spp. In Trinidad *Acarinina densa* occurs in the *Hantkenina aragonensis* and *Globigerapsis kugleri* Zones of Bolli (1957).

Illustrations of some of the microfossils from the samples noted above and in Table 1 are shown in text-figure 8.

Area 3: (text-fig. 4). E-MORB basalt with interbedded pelagic limestone. See "D" in text-figure 4.

At Locality Kh-01-D3-S6 Upper Cretaceous (Zone 2B, uppermost Campanian) planktonic foraminifera were recovered from interbedded indurated micrites in this unit using the Kariminia method of microfossil extraction (Kariminia et al. 2003; Kariminia, in press. *See* Table 1 and text-figure 10 herein). The follow taxa occur in micrite samples from Locality Kh-01-D3-S6: *Globotruncana fornicata*, *G. hilli*, *G. lapparenti*, *G. linneiana*, *G. ventricosa*, *Globotruncanita elevata*, *Globotruncanella havanensis*, *Archaeoglobigerina* sp., and *Heterohelix* spp. Analysis of samples from Texas, Arkansas, Mexico, and Puerto Rico indicate that *Globotruncana hilli* and *Globotruncanella havanensis* both make their first appearance at the base of Zone 2B and *Globotruncana ventricosa* makes its final appearance at the top of Zone 2B. (*See* text-figure 10A). Zone 2 B is equivalent to the *Globotruncana calcarata* Zonule of Pessagno (1967, 1969).

Area 3 (text-fig. 4): Basaltic andesite-subalkaline basalt (N-MORB affinity) with interpillow siliceous mudstone. See "F" in text-figure 5.

At localities Kh-01-D3-S22 and Kh-01-D3-S24 the following Upper Cretaceous (lowermost Coniacian) Radiolaria were extracted from interpillow siliceous mudstone samples utilizing the HF Technique of Pessagno and Newport (1972): *Pseudoaulophacus putahensis*, *Alievium praegallowayi*, *Dictyomitra formosa*, *Dictyomitra torquata*, *Pseudodictyomitra* sp., *Xitus*

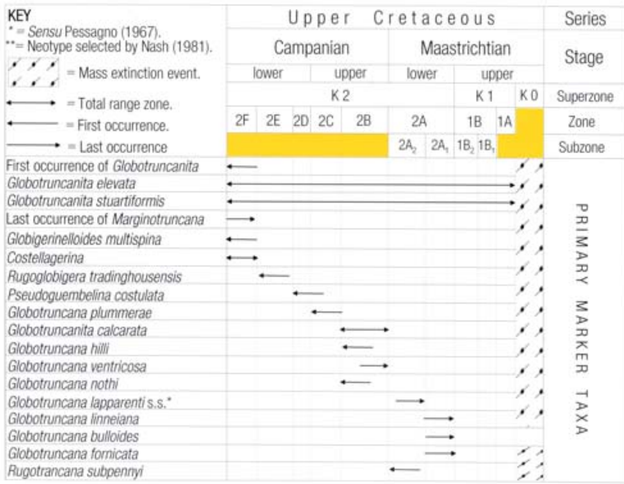

TEXT-FIGURE 10
Planktonic foram zonation for the Campanian-Maastrichtian (part). From Pessagno (in prep.)

sp., *Patellua* sp., and *Orbiculiforma quadrata*(?). This assemblage is assigned to the base of Zone 12, Subzone 12A (Pessagno, 1977; see Figure 11 herein). In the California Coast Ranges Pessagno (1977) determined that *Dictyomitra formosa* and *Alievium praegallowayi* made their first appearance at the base of his Subzone 12A whereas *Pseudodictyomitra* sp. and *Pseudoaulophacus putahensis* make their final appearance at the top of Zone 11, Subzone 11B. In Oman Tippit et al. (1981) found *Pseudodictyomitra* sp. to range into the lower part of Subzone 12. It is likely that the range of *Pseudoaulophacus putahensis* extends into the lower Coniacian although the possibility of reworking can not be ignored.

Text-figure 13 illustrates lowermost Coniacian Radiolaria from this locality.

Area 4 (text-fig. 4): Upper Cretaceous reddish brown, manganiferous ribbon chert overlain (sedimentary contact) by medium to thick bedded pyroclastics (tuff and tuff breccia).

The Radiolarian assemblage from localities Kh-01-D5-S34 and Kh-01-D5-S35 in Area 4 is essentially the same as that in Area 3 ("E") (See Table 1). This assemblage is characterized by the presence of *Dictyomitra formosa* Squinabol, *Dictyomitra torquata* Foreman, and *Pseudodictyomitra* Pessagno. Moreover, it is assignable to Zone 12, lowermost part of Subzone 12: Upper Cretaceous: lowermost Coniacian. See text-figures 11-12 herein.

GEOCHRONOMETRY

^{40}Ar-^{39}Ar ages

The result from incremental heating ^{40}Ar-^{39}Ar age determinations on four hornblende mineral separates from two pegmatitic gabbro (text-figure 4, "B") and two hornblende amphibolite samples (text-figure 4, "A") from rocks in ophiolitic remnants within the "Khoy complex " is presented in Table 2 and text-figures 14-17. Age determinations were calculated in three ways. We first examined age spectra (step ages versus temperature, represented by %^{39}Ar released) for evidence of concordant step ages for a majority of the Ar released from the sample (so-called plateau ages). Good plateaus were apparent in all samples, defining a narrow age range from 156 to 159 Ma for the gabbros and 107-110 Ma for the amphibolite samples. We also calculated total fusion ages obtained by summing all the step compositions, as if the sample had been heated to fusion in one step. These total fusion ages range from 153 to 160 Ma for the gabbro, and from 107 to108 for the amphibolites which are

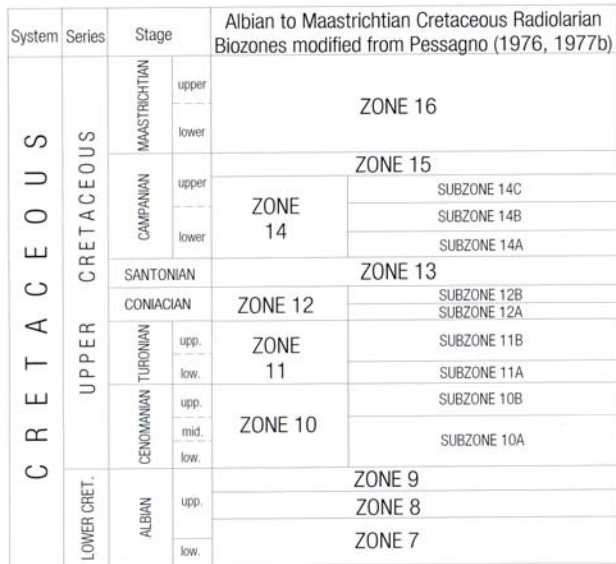

TEXT-FIGURE 11
Albian to Maastrichtian radiolarian biozones modified from Pessagno (1976, 1977). Note that Zone 9 includes Vraconian interval which most workers now place in upper-most Albian. Pessagno (ibid.) previously placed Zone 9 in the lower Cenomanian.

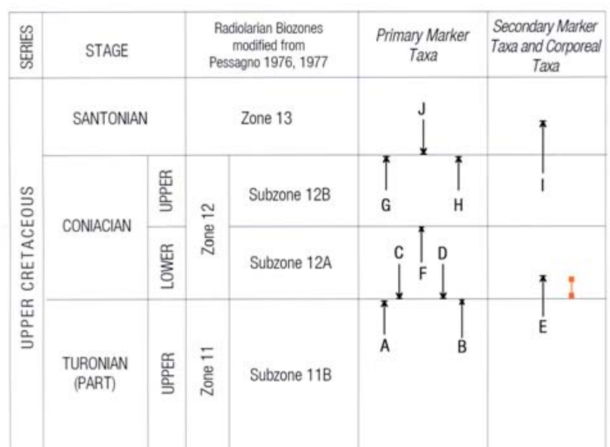

TEXT-FIGURE 12
Upper Cretaceous Radiolarian Biozones and Chronostratigraphic Assignment for the upper Turonian, Coniacian, and Santonian. Modified from Pessagno 1976, 1977. *A = Archaeospongoprunum venadoensis. B = Pseudoaulophacus putahensis. C = Alievium praegallowayi. D = Dictyomitra formosa. E = Alievium superbum. F = Paronaella solanoensis. G = Archaeospongoprunum triplum. H = Orbiculoforma vacaensis. I = Alievium praegallowayi. J = Alievium gallowayi.*

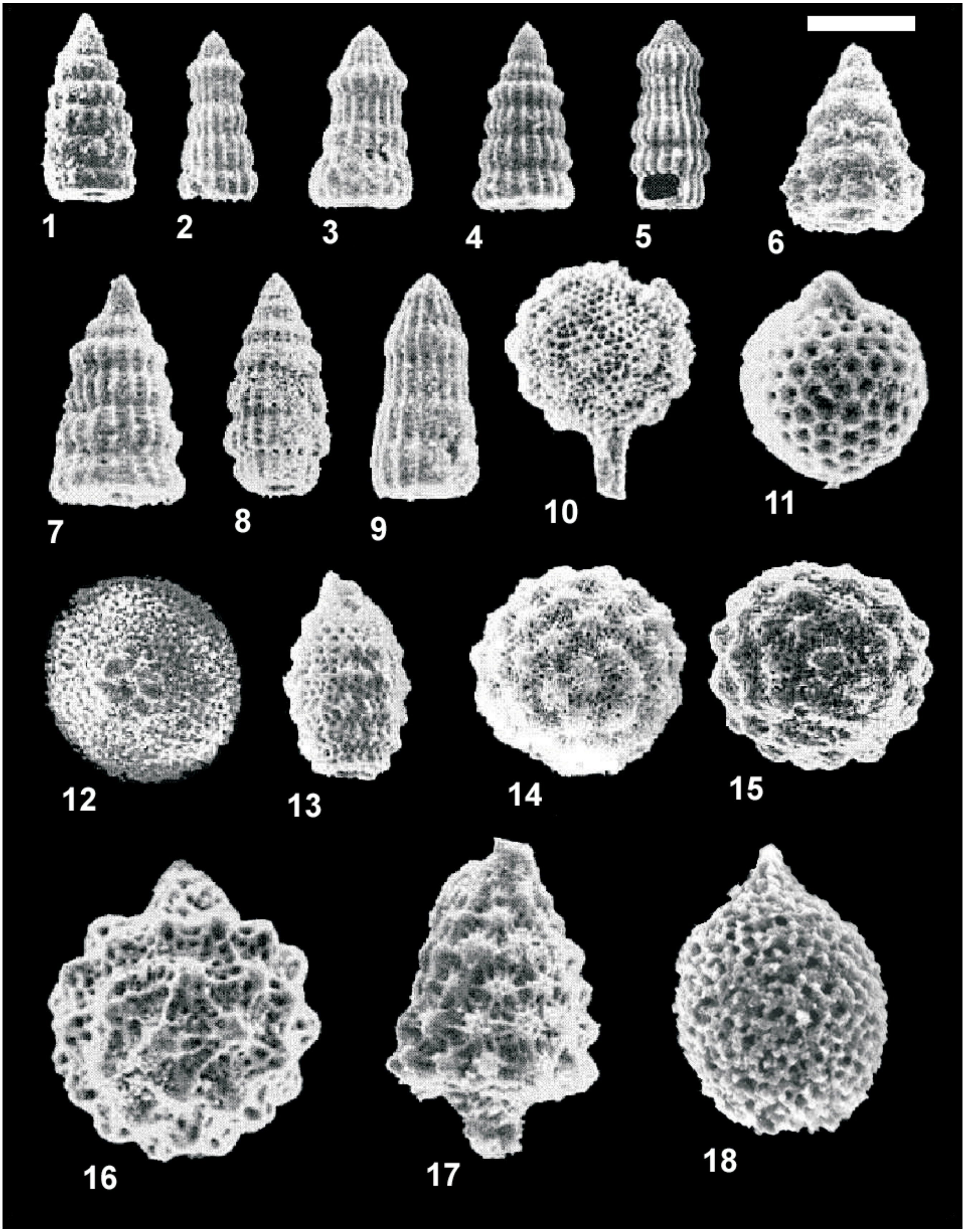

TEXT-FIGURE 13
Upper Cretaceous (lowermost Coniacian) Radiolaria from the Khoy Complex, northwestern Iran.

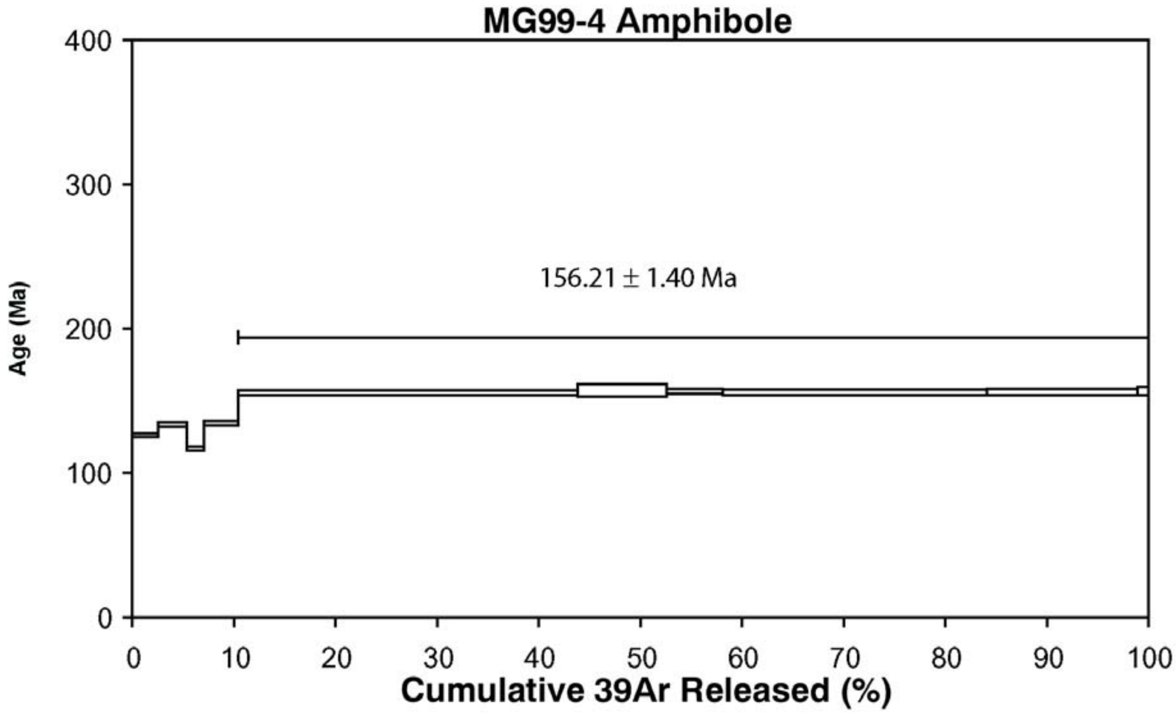

TEXT-FIGURE 14
Late Jurassic (middle Oxfordian) age for gabbro in Area 1. Note that we use the Geologic Society of America 1999 Geologic time scale for geochronologic interpretation of the geochronometric data. Oregon State University sample MG99-4.

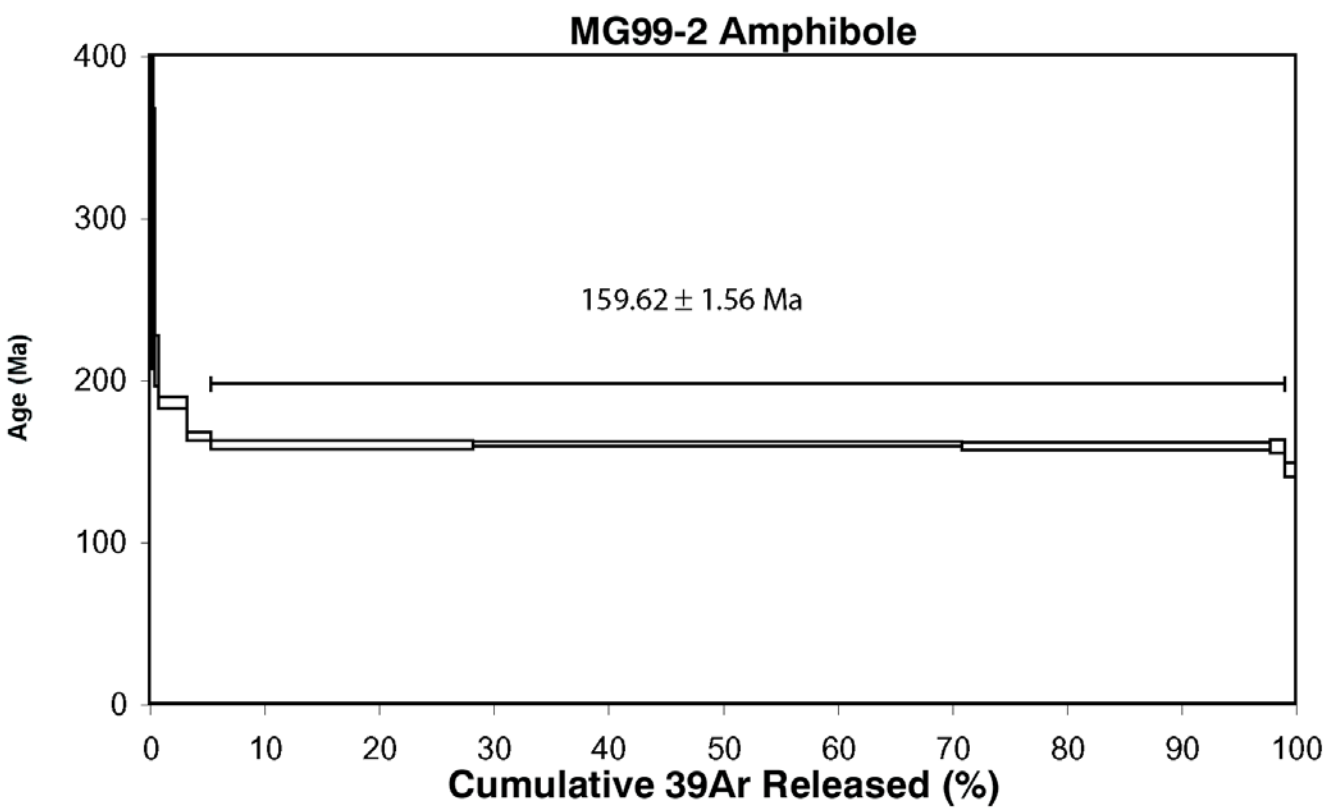

TEXT-FIGURE 15
Late Jurassic (early Oxfordian) age for gabbro in Area 1. Note that we use the Geologic Society of America 1999 Geologic time scale for geochronologic interpretation of the geochronometric data.Oregon State University sample MG99-2.

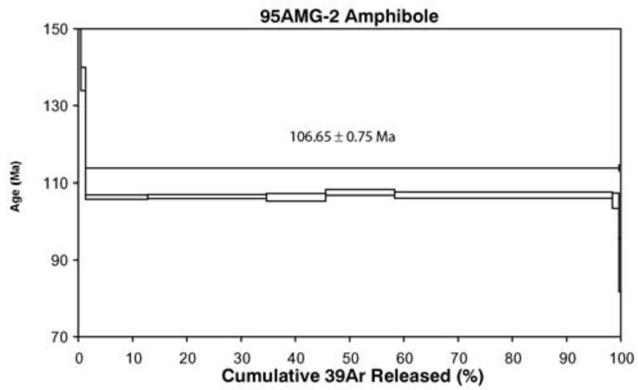

TEXT-FIGURE 16
Early Cretaceous (early Albian) geochronometric data for 95-AMG-2. Using 1999 Geologic "Time" Scale: Geological Society of America. Age on ampibolite (Area 1: text-figure 4).

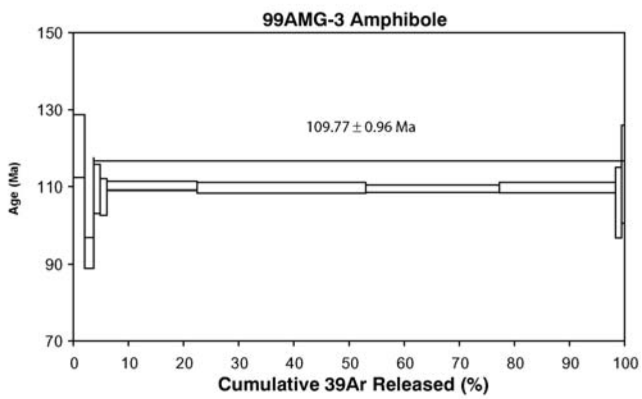

TEXT-FIGURE 17
Early Cretaceous (early Albian) geochronometric data for 99AMG-3. Using 1999 Geologic "Time" Scale: Geological Society of America. Age on amphibolite. See text-figure 4: Area 1.

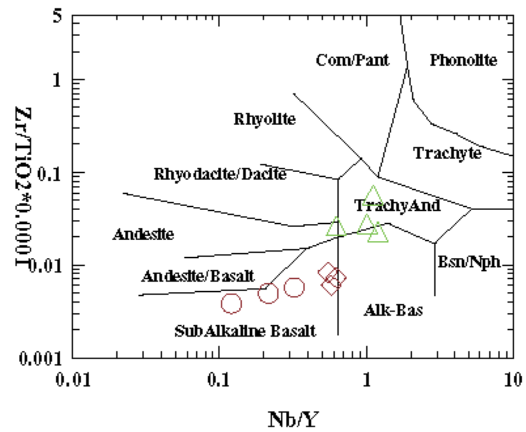

TEXT-FIGURE 18
Zr-Ti-Nb-Y geochemical discrimination diagram (after Winchester and Floyd 1971) showing three types of extrusive rocks.

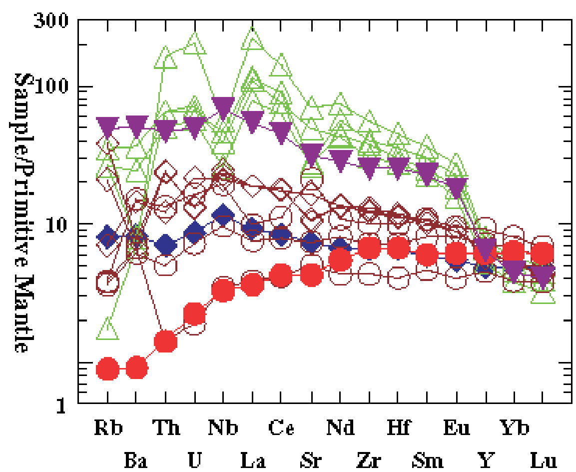

TEXT-FIGURE 19
Incompatible element patterns of extrusive normalized to primitive mantle. Shown for comparison are patterns for typical OIB (solid inverted triangle), MORB (solid circle) and E-MORB (solid diamonds), (Sun and McDonough 1980); Normalizing values for primitive mantle from Sun and McDonough (1989). Andesite-trachyandesites are shown by open triangles, alkalic basalt are shown by open diamond squares and sample of subalkaline basalts are shown by open circle.

comparable to plateau ages. The third age calculation was derived from the correlation of the step Ar compositions ($^{36}Ar/^{40}Ar$ versus $^{39}Ar/^{40}Ar$ isochrons). These correlations allow us to determine the initial composition of Ar in the sample at crystallization, assumed to be atmospheric ($^{40}Ar/^{36}Ar$ = 295.5) in the age spectra calculations. The isochron ages range from 155 to 157 Ma for the gabbro and from 107 to 108 for the amphibolite which are also comparable with both plateau and total fusion ages. Furthermore, for all the samples, the isochrons revealed initial compositions close to the atmospheric values, confirming the reliability of the plateau ages. The isochron ages are concordant with, but have slightly larger fitting uncertainties than, the plateau ages.

GEOCHEMISTRY

Fifteen samples of extrusive rock from the "Khoy complex" were analyzed for geochemical signatures. In general, these volcanic rocks have suffered extensive secondary changes due to sea-floor alteration and low-grade hydrothermal metamorphism. This alteration typically results in losses or gains of most of the major elements. In this report we have focused our attention on the analysis of the ten samples from the extrusives with the least amount of alteration. Based on a Nb/Y vs. Zr/Ti diagram (Winchester and Floyd 1977) the extrusive rocks from the ophiolitic rocks in the "Khoy complex" can be divided into at least three different types (text-figure 18):

Group 1: Andesite-trachyandesite;

Group 2: Basaltic andesite-subalkaline basalt; and

Group 3 Alkalic basalt.

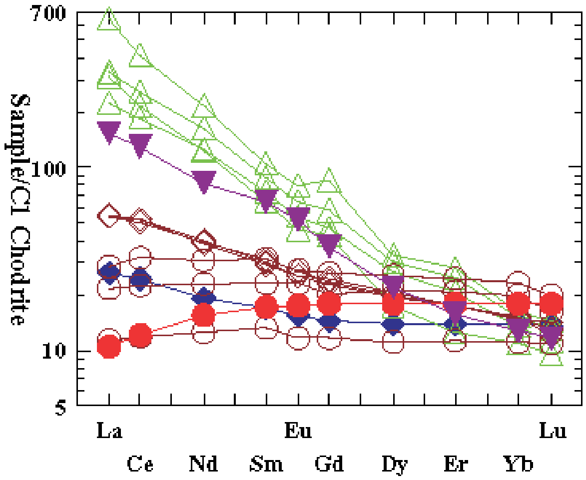

TEXT-FIGURE 20
Rare earth element (REE) patterns of extrusive rocks normalized to C1 Chondrite. Shown for comparison are patterns for typical OIB (solid inverted triangle), MORB (solid circle) and E-MORB (solid diamonds), (Sun and McDonough, 1980); Normalizing values for primitive mantle from Sun and McDonough (1989). Andesite-trachyandesites are shown by open triangles, alkaline basalt are shown by open diamond squares and sample of subalkaline basalts are shown by open circle.

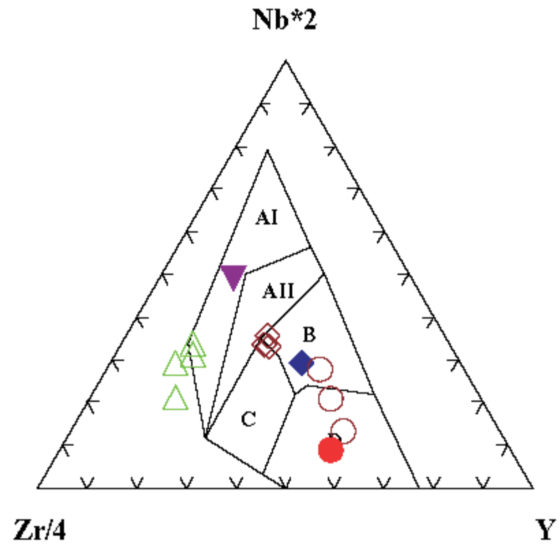

TEXT-FIGURE 21
Chondrite-normalized REE patterns for extrusive rocks the Khoy ophiolite. Normalizing values for Chondrite from Sun and McDonough (1989). Andesite-trachyandesites are shown by open triangles, alkalic basalt are shown by open diamond squares and sample of subalkaline basalts are shown by open circle.

Selected minor and trace elements (e.g., Ti, Zr, Y, Hf and Nb) believed to be relatively immobile under conditions of metasomatism and low-grade hydrothermal metamorphism are used to characterize extrusive rocks with respect to their original composition and possible tectonic environment of formation (e.g., Pearce and Cann 1973; Winchester and Floyd 1977; Pearce 1996; Jenner 1996). In a Zr-Nb-Y discrimination diagram (Meschede 1986), the results from all the extrusive rocks show three distinct chemical affinity. The basaltic andesite-subalkaline groups show N-MORB chemical affinity, whereas the alkaline basalts show within-the-plate type chemical affinity, and the trachyandesite samples plot in the field of within-plate alkalic basalt.

Primitive mantle-normalized incompatible element patterns and chondrite-normalized rare earth patterns (REE) for these extrusive rocks are illustrated in text-figures 19 and 20. For the purpose of comparison the patterns from ocean island basalt (OIB), E-MORB and N-MORB are plotted (Sun and McDonough, 1989). In general, the patterns for these extrusives form three recognizably different semi-parallel envelopes. Patterns for the trachyandesite group have the highest relative abundances, are light REE-enriched and show very good similarities with ocean island basalt. However, the large trough at Nb is a characteristic feature of extrusive rocks influenced by continental lithosphere which has been explained in terms of fractionation and retention of this element in the source during partial melting of the subducting plate (Pearce, 1996). The basaltic andesite-subalkaline basalt have elemental signatures that are similar to those of N-MORB and the samples which were identified as alkalic basalts clearly show E-MORB origin (text-figures 19-21). In general, the preliminary geochemical data show three distinct geochemical signatures (OIB, E-MORB and MORB) for the extrusive rocks from the Khoy ophiolite Complex.

DISCUSSION AND CONCLUSIONS

(1) Biostratigraphic, chronostratigraphic, geochronometric, geochronological, and geochemical data resulting from our investigations indicate that there are at least two and possibly three remnants of oceanic crust within the "Khoy complex": A Late Jurassic (early to middle Oxfordian) remnant (Area 1, "A"); an early Coniacian remnant (Area 3 **"E"**: N-MORB affiliated geochemistry); and, possibly, and, a latest Campanian remnant (Area 3 **"D"**: E-MORB geochemistry) (*See* text-figure 3-4).

(2) Ampibolite closely associated with the Late Jurassic remnant has been dated as Early Cretaceous (early Albian: 107-110 MA ^{40}Ar-^{39}Ar). The amphibolite needs further study. It may be an exotic slab which is totally unrelated to the other ophiolites or may represent a metamorphosed part of the adjacent Late Jurassic remnant.

(3) The crystallization ages of 159.6±1.56 Ma and 156.2±1.4 Ma for the gabbros suggest that ophiolite formation in that part of Neotethys which is now present-day northwestern Iran (in the vicinity of the Caspian sea) began in the Late Jurassic (early to middle Oxfordian). As a consequence, this ophiolite formed much earlier than other ophiolites along the Zagros suture zone. For example, total gas ^{40}Ar-^{39}Ar ages for hornblendes from ophiolitic rocks at the Neyriz ranging from 77±2.4 Ma to 104±1.0 Ma were interpreted by Lanphere and Pamic (1983) to indicate Late Cretaceous age of crystallization for the formation of the Neyriz ophiolite. Similarly, Delaloye and Desmons (1980) obtained K/Ar ages of 86 Ma and 81 Ma for diorite and diabase samples from the Sahneh (Kermanshah) ophiolite of western Iran. The geochronometric age for the Kermanshah Ophiolite is relatively compatible with the early Coniacian determination that the senior author obtained from the analysis of

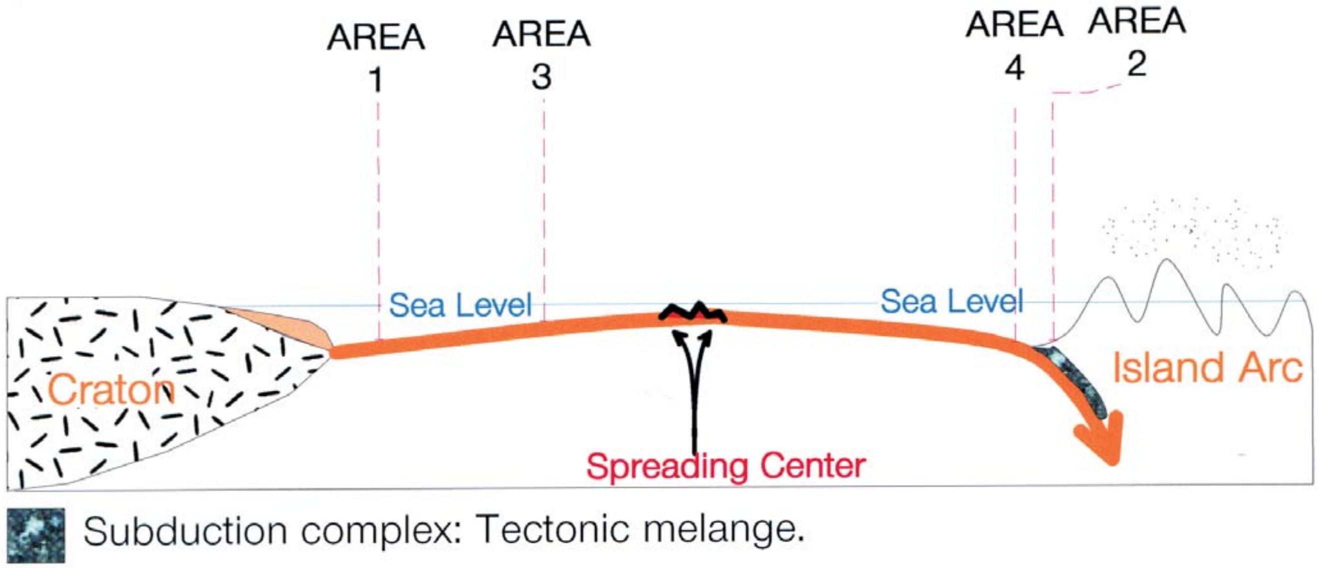

TEXT-FIGURE 22
Reconstruction of components of Khoy Complex, northwestern Iran. Area 1: Early Cretaceous (late Albian) ophiolite with ultramafics, gabbro amphibolite. Includes Late Jurassic (Oxfordian) remnant. No sedimentary rocks known. Area 2: Tectonic mélange containing knockers of pelagic limestone (micrite with radiolaria and planktonic foraminifera), serpentinite,and basalt. Pelagic limestone knockers ranging in age from Early Cretaceous (latest Albian) to Early Middle Eocene. Area 3: E-MORB basalt with interbedded pelagic limestone (micrite) containing Late Cretaceous (latest Campanian planktonic foraminifera. Basaltic andesite-subalkalinepillow lava (N-MORB) with interpillow siliceous mudstone containing Late Cretaceous (early Coniacian) radiolaria. Area 4: Upper Cretaceous red, manganiferous ribbon chert overlain (sedimentary contact) by medium to thick bedded pyroclastics (tuff and tuff breccia). To date, only early Coniacian Radiolaria have been recovered from chert exposures adjacent to and below the pyroclastics.

Kermanshah radiolarian chert associated with the ophiolite. The Neyriz and Sahneh (Kermanshah ophiolite) possibly were coeval with the Semail and other Neotethyan ophiolites of the Bitlis Zagros suture zone (e.g., Sengor 1990).

(4) The assumption by previous workers (e.g., Ghazi and Hassanipak 1996; Ghazi et al. 1997) that the Khoy represents a single ophiolite is invalid because at least two and possibly three different ophiolite remnants are present. These rocks should be included under the term "Khoy complex" (sensu International Stratigraphic Guide).

(5) Our preliminary analysis of remote sensing data indicates that the latest Campanian ophiolite remnant (E-MORB geochemistry) has been juxtaposed against an early Coniacian ophiolite remnant comprised of basaltic andesite-subalkaline basalt (N-MORB) affinity) with radiolarian-rich interpillow mudstone and red ribbon chert (Area 3: See text-figure 4: **"E"**). It is tempting to suggest that the latest Campanian E-MORB basalts are part of the same volcanic sequence that disconformably overlies the red ribbon chert in Area 4 (see below).

(6) The early Coniacian red ribbon chert characteristic of Area 4 represents pelagic strata deposited at or near an oceanic spreading center (See text-fig. 4: F). The contact between the lower Coniacian red chert and overlying pyroclastics (tuff and tuff breccia) represents a disconformity and an associated hiatus of unknown magnitude (text-figure 7). This contact indicates that oceanic crust topped by radiolarian ooze lacking any sort of calc-alkaline island arc components had arrived in the vicinity of an island arc by the early Coniacian or later.

(7) Tectonic mélange present in Area 2 (text-figs. 4, 22) is interpreted to represent a subduction complex associated with an island arc. Biostratigraphic and chronostratigraphic data acquired thus far indicate that subduction was active from the Early Cretaceous (late Albian: Vraconian) until the early Middle Eocene.

(8) Finally, we suggest that the oceanic spreading center, subduction complex, and island arc complex depicted in Figure 22 were abducted on to the craton during post early Middle Eocene time.

ACKNOWLEDGMENTS

This study was supported by National Science Foundation grants (EAR-9903249, EAR-0073966) to Ghazi and by National Science Foundation grant EAR-0074120 to Pessagno and Ghazi respectively. We wish to thank Dr. Robert J. Coleman, School of Earth Sciences, Stanford University, Stanford, California 94305 and Dr. Charles D. Blome, U. S. Geological Survey, Federal Center, Denver, Colorado 80225-0046 for their care in reviewing the manuscript. Contribution number 966, Department of Geosciences, The University of Texas at Dallas.

REFERENCES

BOLLI, H. M., 1957. The genera *Praeglobotruncana*, *Rotalipora*, *Globotruncana* in the Upper Cretaceous of Trinidad, B.W.I. *U.S. National Museum Bulletin*, 215: 51-60, pls. 12-14, fig. 10.

COLEMAN, R. J., 1981. Tectonic setting for ophiolite obduction in Oman. *Journal of Geophysical Research*. (Special Issue), 86: 2497-2508.

DELALOYE M. and DESMONS, J. 1980. Ophiolites and Melange terranes in Iran: a geochronological study and its paleotectonic implications. *Tectonophysics*, 68: 83-111.

TABLE 1
New planktonic foraminiferal and radiolarian biostratigraphic and chronostratigraphic data from the Khoy Complex.
*Foraminifera separated from indurated micrite using method of Kariminia et al. 2003.

SAMPLE	CHRONOSTRATIGRAPHIC DETERMINATION	BIOSTRATIGRAPHIC DETERMINATIONS. SEE FIGURES 7-8	Taxa	Type of microfoss	Area & GPS data (where available). *See Figure 4.*	Rock type
Kh-01-D3-S19-b	lower Campanian - lower Maastrichtian	Zone 2F to Subzone 2A1	*Globotruncana linneiana, Globotruncana bulloides, Globotruncana spp.*	Planktonic Foraminiferida	**AREA 2. "C" in Figure 4. N38°,46', 24.1" E44°,30', 58.3"**	Pelagic Limestone (micrite)
Kh-01-D4-S29	upper Maastrichtian	Subzone 1B1 to upper part of Zone 1A	*Globotruncanita conica, Globotruncanita elevata, Globotruncana navarroensis, Globotruncanella havanensis, Racemiguembelina fructocosa*	Planktonic Foraminiferida*	**AREA 2. "C" in Figure 4. N38°,52', 57.1" E44°,33', 52.5"**	Pelagic Limestone (micrite)
KH 99-46.3	lower Cenomanian	base Subzone 10A	*Pseudodictyomitra pseudomacrocephala, Archaeodictyomitra sliteri, Holocryptocanium astiensis, Thanarla praeveneta, Patelula spp., Alievium* spp.	Radiolaria	**AREA 2. "C" in Figure 4.**	Pelagic Limestone (micrite)
KH 99-46.3	uppermost Albian to lower Cenomanian	Zone 7 to Superzone 6, Zone 6D of Pessagno, in prep.	*Thalmanninella evoluta, Hedbergella planispira, Hedbergella delrioensis*	Planktonic Foraminiferida	**AREA 2. "C" in Figure 4.**	Pelagic Limestone (micrite)
KH 99-21-1-2	lower middle Eocene	Equivalent to Bolli's (1957) *Hantkenina aragonensis* and *Globigerapsis kugleri* zones of Trinidad.	*Acarinina densa, Acarinina* spp.	Planktonic Foraminiferida	**AREA 2. "C" in Figure 4.**	Pelagic Limestone (micrite)
Kh-01-D3-S6	uppermost Campanian	Superzone UK2, Zone 2B	*Globotruncana fornicata, G. hilli, G. lapparenti, G. linneiana, G. ventricosa, Globotruncanita elevata, Globotruncanella havanensis, Archaeoglobigerina sp., Heterohelix spp.*	Planktonic Foraminiferida*	**AREA 3. "D" in Figure 4 N38°,36' E44°,40'**	Pelagic Limestone (micrite)
Composite Kh-01-D3-S22 and Kh-01-D3-S24	lowermost Coniacian	Zone 12, lowermost part of Subzone 12A.	*Pseudoaulophacus putahensis , Alievium praegallowayi , Dictyomitra formosa , Dictyomitra torquata, Pseudodictyomitra* sp., *Xitus* sp., *Patellua* sp., *Orbiculiforma quadrata* ?	Radiolaria	**Area 3."E" in Figure 4. N38°,41', 45.5" E44°,25', 09.1"**	Siliceous mudstone
Kh-01-D5-S34 and Kh-01-D5-S35	lowermost Coniacian	Zone 12, lowermost part of Subzone 12A.	Same fauna as Kh-01-D3-S22, 24 above	Radiolaria	**AREA 4. "F" IN Figure 4. N38°,58', 45.9" E44°,12', 9.6" and N38°,59', 7.3" E44°,12', 10.2" respectively**	Medium to thin-bedded reddish brown chert

DESMONS, J. and BECCALUVA, L. 1983. Mid-oceanic ridge and island arc affinities in ophiolites from Iran: Paleogeographic implication. *Chemical Geology*, 39: 39-63.

DEWEY, J.F. and BIRD, J.M., 1970. Mountain bets and the new global tectonics. *Journal of Geophysical Research,* 75: 2625-2647.

DILEK, Y. and MOORES, Y. 1990. Regional tectonics of the eastern Mediterranean ophiolites. In: J. Malaps, Moores, E.M., Panayiotou, A. and Xenophonotos, C., Eds., Ophiolites, Oceanic Crustal Analogues. *Proceedings of the Symposium "Troodos 1987",* Geological Survey, Nicosia, Cyprus. 295-309.

DILEK, Y., and DELALOYE, M., 1992. Structure of the Kizidag ophiolite, a slow-spread Cretaceous ridge segment north of the Arabian promontory. *Geology*, 20: 19-22.

GHAZI, A.M. and HASSANIPAK, A. A., 1995. Petrogenesis and tectonic setting of the Band Ziarat ophiolite, southern Iran. *Abstracts with Program,* Geological Society of America: 27, 435.

GHAZI, A.M. and HASSANIPAK, A. A., 1996. Geochemistry and petrology of the Kermanshah ophiolite, southwest Iran. *Abstracts with Program,* Geological Society of America , 28: 481.

GHAZI, A.M. and HASSANIPAK, A. A., 1996. Geochemistry, petrology and preliminary K/Ar ages of the Khoy ophiolite, northeastern Iran: Implications for Tethyan tectonics. *EOS, Transactions American Geophysical Union*, 78: F836.

GHAZI, A.M., HASSANIPAK, A.A., DUNCAN, R.A., HOGEN, L.G. and MAHONEY, J.J., 1997. Geochemistry, $^{40}Ar/^{39}Ar$ ages and preliminary isotopic analyses of the Khoy Ophiolite, northwestern Iran. *EOS, Transactions American Geophysical Union,* 78**:** F654.

GHORASHI M. and ARSHDI S. (compilers), 1978. Geological maps of Khoy Quadrangle, scale, 1:250,000. *Geological Survey of Iran*.

INTERNATIONAL SUBCOMMISSION ON STRATIGRAPHIC CLASSIFICATION, 1976. International stratigraphic guide, Hedberg, H. D., Ed., *A guide to stratigraphic classification, terminology, and procedure.* New York: John Wiley and Sons, 200 pp.

JENNER, G. J., 1996. Trace element geochemistry of igneous rocks: geochemical and nomenclature and analytical geochemistry. In: Wyman, D. A., Ed., Trace element geochemistry of volcanic rocks: Applications for massive sulphide exploration. *Geological Association of Canada, Short Course Notes No.12*, 51-78

KARAMINIA, S. M., PESSAGNO, E. A., JR., CARTER, J. L., and SABETI-SORAIADOOST, N., 2003. Extraction of calcified Radiolaria and other calcareous microfossils from micritic limestone utilizing acetic acid. *Geological Society of America Abstracts with Programs,* 35 (7): 495.

KARIMINIA, S. M., in press. Extraction of calcified Radiolaria and other calcified microfossils from micritic limestone utilizing acetic acid. *Micropaleontology*, 12 p. MS., 4 text-figures, 2 pls.

LANPHERE, M.A. and PAMIC, T., 1983. $^{40}Ar/^{39}Ar$ Ages and Tectonic Setting of Ophiolites from Neyriz area, South-east Zazros ranges, Iran. *Tectonophysics*, 96: 245-256.

MESCHEDE, M., 1986. A method of discriminating between different types of mid-ocean ridge basalts and continental tholeiites with the Nb, Zr, Y diagram. *Chemical Geology* 56, 207-218.

MOORES, E.M., and VINE, F., 1971. The Troodos massif, Cyprus and other ophiolites as oceanic crust: evaluation and complications. *Transactions of the Royal Society of London,* 268: 433-466.

MOORES, E.M., ROBINSON, P.T., MALAPS, J. and XENOPHONOTOS, C., 1984. Model for the origin of the Troodos massif, Cyprus, and other mideast ophiolites. *Geology*, 12: 500-503.

NICOLAS, A. and BOUDIER, F., 1991. Rooting of the sheeted dike complex in the Oman ophiolite. In: Peters Tj., Nicolas A. and Coleman R.G., Eds., *Ophiolite Genesis and evolution of the Oceanic Lithosphere*. Kluwer Academic Publisher, 39-54.

PEARCE, J.A. and CANN, J.R. 1973. Tectonic setting of basic volcanic rocks determined using trace element analyses. *Earth and Planetary Science Letters,* 19: 290-300.

PEARCE, J. A., 1996. A user's guide to basalt discrimination diagrams. In: Wyman: D.A., Ed., Trace element geochemistry of volcanic rocks: Applications for massive sulphide exploration. *Geological Association of Canada, Short Course Notes*, 12: 79-113.

TABLE 2
^{40}Ar-^{39}Ar measurements of hornblende separates in gabbros and amphibolites from the Khoy ophiolite complex. Note that samples are from Area 1, "A". See text-figure 4 herein.

Sample	TFA	WMPA	IA (Ma)
Gabbro: MG99-2	160.99	159.6±1.56	157.6±4.6
Gabbro: MG99-4	153.27	156.2±1.40	153.3±1.40
Amphibolite:MG99-3	107.8	109.77±0.96	107.6±6.6
Amphibolite: MG99-2	108.2	106.65±0.75	107.2±1.4

Notes: TFA-total fusion age: IA-isochron age: WMPA: weighted mean plateau age. All errors are 2Φ.

PESSAGNO, E. A., JR., 1976. Radiolarian Zonation and Stratigraphy of the Upper Cretaceous Portion of the Great Valley Sequence. *Micropaleontology*, Special Paper 2: 1-95, 10 text-figs, 14 pls.

PESSAGNO, E. A., JR., 1977. Lower Cretaceous Radiolaria and Radiolarian biostratigraphy of the Great Valley Sequence and Franciscan Complex, California Coast Ranges. *Cushman Foundation for Foraminiferal Research, Special Paper* 15: 1-87, 12 pls., 8 figs.

PESSAGNO, E. A., JR. AND NEWPORT, R. L., 1972. A technique for extracting Radiolaria from radiolarian cherts, *Micropaleontology*, 18 (2): 231-234, 1 plate.

SARKARINEJAD, K. 1994. Petrology and tectonic settings of the Neyriz ophiolite, southeast Iran. In: Ishiwatari, A., et al., Circum-Pacific Ophiolites. *Proceeding of the 29th International Geological Congress, Part D,* 221-234.

SENGOR, A.M.C., 1990. A new model for the late Paleozoic-Mesozoic tectonic evolution of Iran and implications for Oman. In: Robertson, A. H. F., Searle, M. P. and Ries, A. C., Ed., The Geology and Tectonics of the Oman Region. *Geological Society of London Special Publication,* 49: 797-831.

STOCKLIN, J., 1974. Possible ancient continental margin in Iran. In: Burk C. A. and Drake C. L., *The geology of continental margins*. New York: Springer-Verlag, 873-887.

SUN, S. S. and MCDONOUGH, W.F., 1989. Chemical and isotopic systematics of ocean basalts: Implication for mantle composition and processes. In: Saunders, A.D. and Norry, M. J., Ed., *Magmatism in Ocean Basins.* Geological Society of London Special Publication, 42: 313-345.

TAKIN, M., 1972. Iranian geology and continental drift in the Middle East. *Nature*, 235: 147-150.

TIPPIT, P. R., PESSAGNO, E. A., JR. and SMEWING, J. D., 1981. The biostratigraphy of sediments in the volcanic unit of the Samail Ophiolite. *Journal of Geophysical Research,* 86(B4): 2756-2762.

WINCHESTER, J.A. and FLOYD, P.A., 1977. Geochemical discrimination of different magma series and their differentiation products using immobile elements. *Chemical Geology,* 20: 325-342.

Manuscript received March 10, 2004
Manuscript accepted October 1, 2004